Radiotherapy and Oncology, 12 (1988) 129–140
Elsevier

RTO 00467

Optimization of stationary and moving beam radiation therapy techniques*

Anders Brahme

Department of Radiation Physics, The Karolinska Institute and University of Stockholm, Box 60204, S-104 01 Stockholm, Sweden

(Received 30 April 1987, revision received 16 August 1987, accepted 22 January 1988)

Key words: Conformation therapy; Computed dose planning; Treatment optimization

Summary

A new approach is suggested for the optimization of stationary and more general moving beam type of irradiations. The method reverses the order of conventional treatment planning as it derives the optimum incident beam dose distributions from the desired dose distribution in the target volume. It is therefore deterministic and largely avoids the trial and error approach often applied in treatment planning of today. Based on the approximate spatial invariance of the convergent beam point irradiation dose distribution, the desired dose distribution in the target volume is analyzed in terms of the optimum density of such point irradiations. Since each point irradiation distribution is optimal for the irradiation of a given point and due to the linearity of individual energy depositions or absorbed dose contributions, the resultant point irradiation density will also generate the best possible irradiation of an extended target volume when the maximum absorbed dose at a certain distance from the target should be minimized. The optimum shape of the incident beam for each position of the gantry is obtained simply by inverse back projection of the point irradiation density on the position of the radiation source for that orientation of the incident beam.

Introduction

Current treatment planning procedures generally employ a trial and error type of approach in testing various beam combinations in order to find the best irradiation technique for a given target volume. In this investigation the reverse approach has been taken, that is: given the desired dose distribution in the target volume, how should the incident beams best be shaped in order to generate this distribution? The optimal dose delivery for many targets in the trunk is of the conformation-convergent beam irradiation type using as many incident directions as possible, considering the shape of the body and the location of eventual organs at risk. These treat-

Address for correspondence: Anders Brahme, Department of Radiation Physics, The Karolinska Institute and University of Stockholm, Box 60204, S-104 01 Stockholm, Sweden.

* This paper is based on material presented at the annual meeting of *ESTRO*, 1985 and 1986.

ment techniques will therefore be studied here in some detail.

Conformation and more general moving beam treatments can today be performed effectively by at least four different irradiation techniques. (1) The most effective is perhaps by using a computer controlled multileaf collimator which can be programmed to follow the projection of the target volume during the rotation of the gantry around the patient. (2) Alternatively the patient can be moved axially while being irradiated by a dynamically controlled slit field also delivered by a rotary gantry [2]. (3) A third alternative is to use a treatment unit with individual collimator jaw movements which can scan a slit field across a stationary patient at the same time as the perpendicular jaws are following the target volume. (4) The fourth approach is to have a generally opened collimator and scan a narrow pencil beam of high energy photons, electrons or protons over the target volume to obtain the best possible dose distribution in each orientation of the gantry.

Naturally all these procedures may be combined in different ways to further optimize the treatment. However, today the multileaf collimator approach is the predominant technique for conformation therapy with the incident beam in its simplest form just shaped to conform with the target contour in each orientation of the gantry. The optimal setting of the multileaf collimator in stationary beam radiation therapy has been treated in a previous publication [3].

For a small target volume, a convergent beam irradiation from all directions will give the highest dose to the target for a given acceptable absorbed dose level in the surrounding normal tissues. A fundamental problem in moving beam dose planning is therefore to determine the most advantageous irradiation technique in order to treat a given extended target volume. This technique should preferably generate the optimal dose distribution inside the target volume [8], and at the same time give minimal dose to surrounding normal tissues. A general and powerful method is developed below to derive the optimal dose delivery using dynamic beam compensation and multileaf collimation during stationary and moving beam therapy. The method is based on a systematic application of the well known optimal dose distribution for the irradiation of small convex target volumes by using Fourier transform techniques or iterative solutions of a Fredholm equation of the first kind.

Optimal dose delivery for small target volumes

The three dimensional converging beam irradiation of a small target volume may be approached in four different steps of increasing comparability with the isotropic spherical irradiation. (1) The first "one" dimensional step is to use parallel opposed fields whereas (2) the second two dimensional step corresponds to a 360° arc treatment in one plane. (3) This later case can be improved by giving a number of additional plane irradiations at an angle to the first one or by conically convergent beams that can be easily produced, for example, using a multileaf collimator. (4) The fourth step is a true isotropic spherical irradiation which may be approached by using multicobalt treatment units or intracranial irradiations with multiple external bremsstrahlung beams. A more strict realization of the isotropic case is obtained using a distribution of internal radiation sources in brachytherapy. To get an idea of the obtainable dose distributions, approximate analytical expressions for these main configurations will first be derived.

(1) The central axis depth-dose distribution in a single photon beam is accurately described by the function:

$$d(z) \propto (e^{-\mu_p z} - ve^{-\mu_e z})\, D_0 \qquad (1)$$

where μ_p is the practical attenuation coefficient of the photon beam, μ_e is the "attenuation" coefficient of the secondary electrons and v being a measure of the electron contamination of the beam [6]. The second exponential thus describes the dose build-up and the first exponential the fall off of the absorbed dose beyond the build-up region [7,13]. The result-

ant central axis dose distribution in the case of two parallel opposed beams of equal weight on a spherical phantom with the crossection 2 r_0 (see Fig. 1) thus becomes:

$$d_p(r) = D_0 \cdot \frac{e^{-\mu_p(r_0+r)} - ve^{-\mu_e(r_0+r)} + e^{-\mu_p(r_0-r)} - ve^{-\mu_e(r_0-r)}}{2(e^{-\mu_p r_0} - ve^{-\mu_e r_0})} \quad (2a)$$

where the denominator normalizes the dose to D_0 in the center of the phantom. By using hyperbolic functions this expression may be reduced to:

$$d_p(r) = D_0 \cdot \left[\cosh\mu_p r - \frac{\cosh\mu_e r - \cosh\mu_p r}{\frac{1}{v} e^{(\mu_e-\mu_p)r_0} - 1}\right] \quad (2b)$$

The first term inside the brases describes the gross dose distribution disregarding effects of the electron build-up, which is taken into account by the last term.

(2) and (3) The two dimensional dose distribution in the plane where the beam is rotated one revolution may be calculated using the previous result. Assuming that the beam is uniform over $2a$ and that the penumbra is negligible (see Fig. 1, for an exact solution see Brahme et al. [6]) the absorbed dose at a given point r, can be calculated from the angular interval φ, under which it is being irradiated. The resultant dose distribution for the cylindrical irradiation becomes:

$$d_c(r) = d_p(r) \frac{2}{\pi} \arcsin\left|\frac{a}{r}\right| \quad (3)$$

(4) Similarly, the dose distribution for the spherically irradiated target is obtained by using the ratio of the spatial angles ($\Omega/2\pi$) in analogy to the previous case:

$$d_s(r) = d_p(r)\left(1 - \sqrt{1 - \left|\frac{a}{r}\right|^2}\right). \quad (4)$$

Due to the close analogy in theoretical approach and its importance in brachytherapy, it is of interest to compare the above dose distribution obtained by irradiation with external beams with the corresponding dose distribution generated by internal radiation sources. The dose distribution around an internal rotationally symmetric and uniform radionuclide distribution of radius a and effective attenuation coefficient μ_p is in the first approximation (neglecting multiple scatter) given by:

$$d_i(r) = D_0 \left|\frac{a}{r}\right|^2 e^{\mu_p(a-r)}. \quad (5)$$

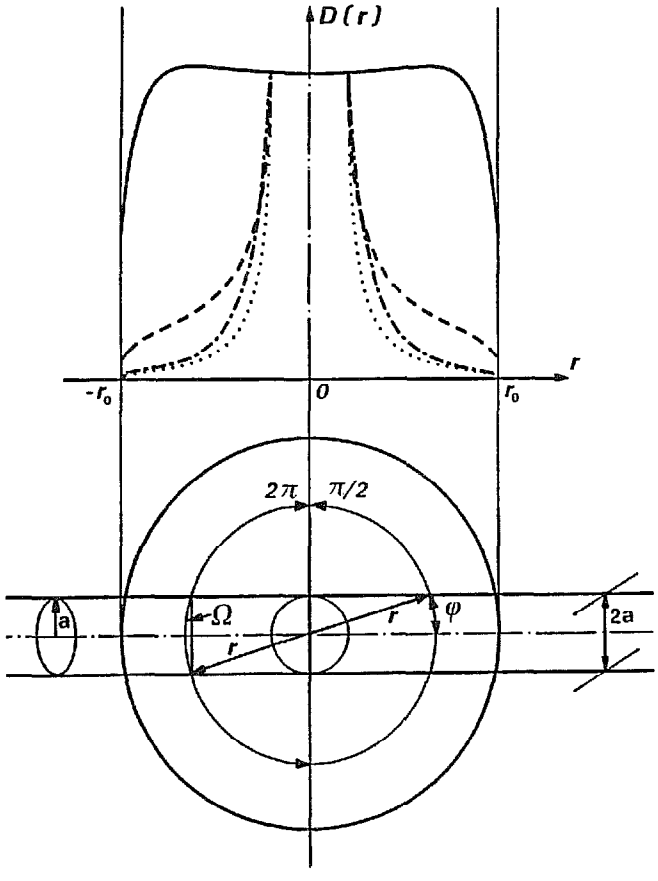

Fig. 1. The coordinate system and typical dose distributions for one dimensional, parallel opposed (——), two dimensional, cylindrical (– – – –) and three dimensional, spheric (.....) treatments of a small target volume. It is seen that a considerable reduction of the normal tissue dose can be achieved by non-coplanar irradiations. In the cylindrical case, the incident slit beam has a width of $2a$ (right half of figure) and for the spherical irradiation the incident beam is circular with radius a (left). The dose distribution with a spherical distribution of radionuclei (–.–.–) is also included for comparison.

The last four dose distributions hold only for $r \geqslant a$, inside a the dose distribution will be practically uniform and close to D_0 in the first approximation as seen by the solid, dashed, dotted, and dash-dotted curves, respectively in Fig. 1. In order to achieve an exactly uniform dose inside a, with external beams the incident beam should ideally be cosine distributed in the plane of rotation according to $d(y) = \cos \mu_p y$, where y is the lateral coordinate in the beam [6]. For internal emitters, the optimum nuclide density distribution may be accurately calculated using Eqns. (12) or (13) below (cf. also Davison [11]).

These four distinct cases, illustrated in the upper half of Fig. 1 show an increasing reduction of the relative dose level outside the target as the beam is distributed over a larger and larger fraction of the spatial angle. The distance from the beam edge to the 50% isodose level is 41.4 and 15.5% respectively of the field half width a for the cylindrical and spherical irradiation respectively. The dose distribution with internal γ-emitters is quite close to the spherical case due to the small μ_p value used for all beams (10 MV). With appropriate internal β-emitters an even better confinement of the irradiated volume is of course possible.

When more accurate results are desirable including effects of phantom scatter and the transport of secondary charged particles, the elementary convergent point irradiation distributions should be measured or calculated using, for example, the Monte Carlo-method. It will be even more accurate to use the basic point spread functions $h(\vec{r})$ already calculated for dose planning purposes [1] and using convolution techniques to determine the appropriate elementary distributions to reduce the Monte Carlo-noise. The point-spread function $h(\vec{r})$ is defined as the ratio of the mean energy imparted per unit volume at a point $\vec{r}$ by the photon energy interacting at the origin ($\vec{r} \equiv 0$). Thus the photon pencil beam dose distribution $p(\vec{r})$ is obtained from the integral:

$$p(\vec{r}) = \int e^{-\bar{\mu}|\vec{z}|} h(\vec{r} - \vec{z})\, dz \qquad (6)$$

where $\bar{\mu}$ is the mean attenuation coefficient and $h(\vec{r})$ is the corresponding point spread function of the incident photon beam and $\vec{z}$ is the depth coordinate along the beam. Pencil beam dose distributions have previously been used for dose planning purposes by some workers [17,21]. From the pencil beam distribution, the cylindrical convergent point irradiation distribution can be expressed as closed line integrals over the pencil beam distribution along circles centered on the pencil beam at the point of convergence [6]:

$$d_c(r) = \oint_r p(\vec{r})\, dl/2\pi r. \qquad (7)$$

Similarly, the dose distribution for a spherically irradiated point is obtained from closed surface integrals over spheres centered on the pencil beam at the point of convergence:

$$d_s(r) = \oint_r \oint p(\vec{r})\, dA/4\pi r^2. \qquad (8)$$

Through the integrations above the possible Monte Carlo-noise in the point spread function $h(\vec{r})$ will be reduced by one to two orders of magnitude and the resultant distributions Eqns. (7) and (8) are well behaved accurately known smooth functions [6].

Extended convex targets without specific organs at risk

The above given basic functions describing the converging isotropic, cylindrical [Eqn. (7)] and spherical [Eqn. (8)] point irradiations are the best possible absorbed dose distributions depending on if a two dimensional or a true three dimensional irradiation technique respectively is desired. Of course, they only pertain to the eradication of small point-like target volumes when there are no specific extra sensitive organ at risk in the vicinity. This is obvious as by distributing the incident beams equally over all angles the maximum absorbed dose at a given distance from the target is minimized. Due to the linearity between absorbed dose and the contrib-

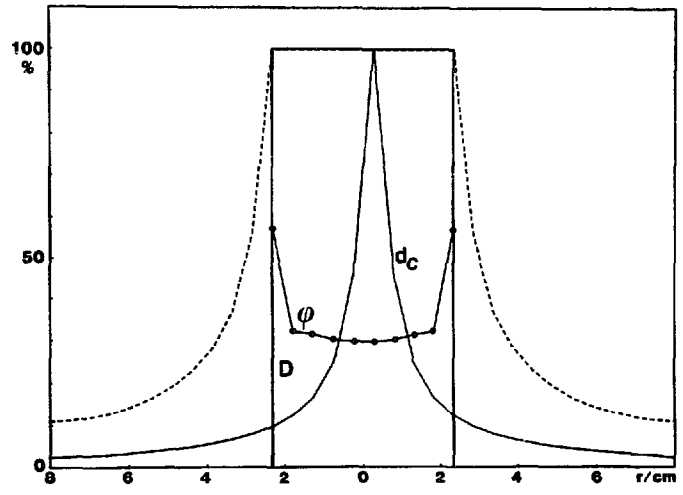

Fig. 2. One dimensional example of the interrelation between the point irradiation density, φ, the cross-sectional shape of an cylindrical isotropic convergent point irradiation dose distribution for 10 MeV photons, d_c [Eqn. (7)], and the desired dose distribution D. ---- is obtained by adding 10-point irradiation dose distributions (d_c) of an amplitude defined by ● on the point irradiation density curve (φ). It is seen that a very good realization of the desired dose distribution is achieved, in this case by using an iterative algorithm [15].

uting energy depositions the superposition principle implies that the optimal dose distribution in an extended volume may be subdivided in the basic optimal distributions for each constituent point-like target. The resultant dose distribution is optimal in the meaning that for a given desired dose distribution in the target volume the maximum absorbed dose at a given distance from the tumor is as small as possible.

Furthermore, as the above convergent point irradiation distributions are primarily determined by the convergent beam geometry and not by photon absorption [see e.g. Eqns. (2–5)] they are very weakly depending on the detailed cross-section and internal structures of the patient or the phantom and may therefore in the first approximation be regarded as spatially invariant. This fact has been well known in conventional arc therapy with finite beams [12,19,22]. To further minimize the effects of this approximation a correction will be introduced in the final reverse back projection [Eqn. (15)] to reduce the errors to second order.

The invariance of $d(\vec{r})$ opens up interesting methods for determining the best possible irradiation technique in order to obtain a desired dose distribution $D(\vec{r})$ in the tumor. One may ask: How should the density $\varphi(\vec{r})$ of convergent point irradiations, each generating a dose distribution $d(\vec{r})$, be chosen to generate the desired target dose distribution $D(\vec{r})$? If φ was known D could be calculated simply by folding φ by g according to:

$$D(\vec{r}) = \int_{V_t}\int\int \varphi(\vec{r}_c)\, d(|\vec{r} - \vec{r}_c|)\, d^3r_c \qquad (9)$$

where $\vec{r}_c$ is the center coordinate of each point irradiation and d could be taken either from Eqns. (3) or (4) using a small value of a, or preferably from Eqns. (7) and (8) which are more accurate. The former equation in each case should be used in the two dimensional case with isotropic cylindrical irradiations and the latter when a true three dimensional irradiation technique is emploied. Thus, φ is given implicitly by an integral equation containing D and r. This equation is illustrated in Fig. 2 for a uniform one dimensional target by discretization of the integral into a sum of 10 terms. Because d in the first approximation is spatially invariant and as there are no extra sensitive organs at risk in the neighborhood of the target volume V_t, the above folding operation may be transformed to a product by Fourier transform of Eqn. (9) according to:

$$\tilde{D}(\vec{s}) = \tilde{\varphi}(\vec{s}) \cdot \tilde{d}(\vec{s}) \qquad (10)$$

where $\tilde{D}$, $\tilde{\varphi}$ and $\tilde{d}$ are the Fourier transforms of the corresponding spatial distributions D, φ and d respectively and $\vec{s}$ is the corresponding spatial frequency according to:

$$\tilde{D}(\vec{s}) = F\{D(\vec{r})\} = \int_{-\infty}^{+\infty}\int\int D(\vec{r})\, e^{-2\pi i \vec{r}\cdot\vec{s}}\, d^3r. \qquad (11)$$

From Eqn. (10), it is seen that the density $\tilde{\varphi}$ in Fourier space is given by the ratio of $\tilde{D}$ and $\tilde{d}$ so after an inverse transform φ can be obtained from the expression:

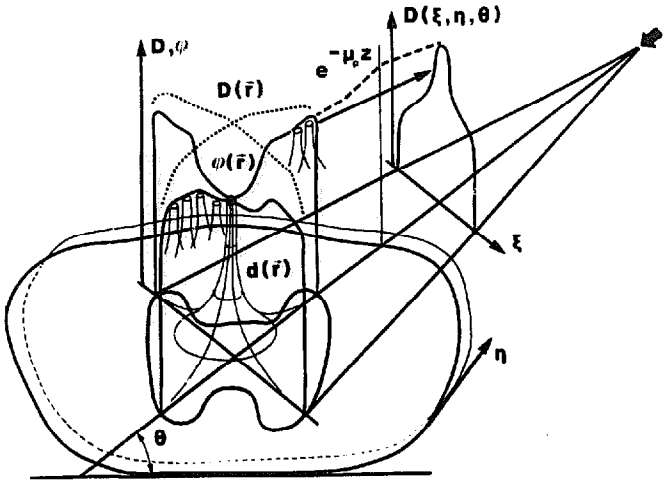

Fig. 3. Schematic illustration of the decomposition of a desired dose distribution $D(\tilde{r})$ in a density distribution $\varphi(\tilde{r})$ of convergent point irradiation distributions $d(\tilde{r})$. The optimal incident beam during moving beam therapy $D(\xi,\eta,\theta)$ is obtained by inverse back-projection of the point irradiation density $d(\tilde{r}_s - \tilde{r}) \cdot \varphi(\tilde{r})$ into the effective radiation source.

$$\varphi(\tilde{r}) = F^{-1}\left\{\frac{\tilde{D}(\tilde{s})}{\tilde{d}(\tilde{s})}\right\}. \tag{12}$$

For numerical calculations, Eqn. (12) may not be ideally suited as the zeros of $\tilde{d}$ will generate very intense high frequency components that results in considerable oscillations in $\tilde{\varphi}$ [14]. These oscillations may be removed or significantly reduced by introducing a low pass filter function $Z(\tilde{s},\lambda)$ in Fourier space according to:

$$\varphi_\lambda(\tilde{r}) = F^{-1}\left\{Z(\tilde{s},\lambda)\,\frac{\tilde{D}(\tilde{s})}{\tilde{d}(\tilde{s})}\right\} \tag{13}$$

A useful form of the filter function Z is:

$$Z(s,\lambda) = \frac{1}{1 + \lambda|\tilde{d}(\tilde{s})|^{-2}} \tag{14}$$

as discussed in more detail by Davies [11] and Lind and Brahme [14]. An alternative approach is to solve Eqn. (9) by iterative procedures as discussed in connection with Eqn. (16) below and by Lind and Brahme [15].

When a practical solution φ_λ has been found by either of these methods, the next step will be to find a suitable realization of this density distribution of basic point irradiations. A natural approach would be to decompose the point irradiation distributions in their constituent pencil beams (Fig. 3) and make "inverse back projections" or simply projections of $d \cdot \varphi_\lambda$ on the effective radiation source at $\tilde{r}_s$, taking into account the true patient geometry and the integrated point irradiation density along the direction of each line integral, l according to:

$$D(\xi,\eta,\theta) = \int_l d(\tilde{r}_s - \tilde{r})\,\varphi_\lambda(\tilde{r})\,e^{\mu_p z(\tilde{r})}\,dz \tag{15}$$

where $D(\xi,\eta,\theta)$ is the resultant transversal dose distribution of the incident beam, $z(\tilde{r})$ is the depth of a point $\tilde{r}$ in the target volume in the direction of projection of the line integral and ξ and η are the transverse co-ordinates of the incident beam perpendicular and parallel, respectively to the rotation axis (Fig. 3). As seen from the figure and Eqn. (15), the incident dose distribution will have a high value where the beam passes a long distance through the target volume or where φ has a high value. This is the case near the central axis in the direction θ chosen to illustrate the line integral in Fig. 3. When the beam is incident from above the reverse is true as seen from the shape of the target volume and the irradiation density (Figs. 3 and 4). The execution of the presently suggested irradiation technique therefore has many resemblances to the back-projections used in computed tomography [6] as seen in Fig. 4 where the incident beams from the upper hemisphere are shown schematically at 45° intervals. The resultant isodose distribution is shown in Fig. 5. Due to the finite voxel size used in the calculation, the desired dose distribution is defined by the jagged line. An almost perfect agreement is seen inside the target volume at the same time as the absorbed dose outside the target is rapidly brought to low values.

The correction for beam absorption in Eqn. (15) during back-projection is expressed by the term $e^{\mu_p z}$. This term ensures that the back-projected beams when used for treatment will generate point

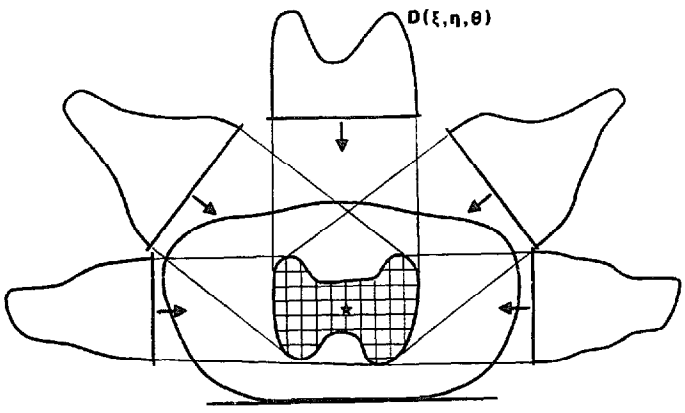

Fig. 4. Schematic illustration of the type of dose delivery that will give the desired dose distribution in the target volume (shaded) and at the same time minimal dose to surrounding normal tissues. The angular dependent dose distributions are most effectively generated using scanned photon beams [5,14,15,18]. For simplicity, the corresponding dose distributions from below are left out in the figure. The location of isocenter (star) is rather uncritical for the present irradiation technique.

irradiation distributions which are practically equal to the initially assumed point irradiation distributions at least inside a radius equal to the shortest distance from the point in question to the nearest significant inhomogeneity in the patient. For a strongly heterogeneous patient, the simple exponential factor should be replaced by a raytrace through the intervening tissues. In practise, this procedure therefore considerably relaxes the need for the isotropic point irradiation distribution to be spatially invariant as assumed above in Eqn. (9).

When $\varphi(\vec{r})$ is a slowly varying function over the target volume or more exactly when $D(\xi,\eta,\theta)$ is rather independent of θ, the optimal irradiation in the above meaning is of the conventional conformation type (see Figs. 4 and 7). When this is no longer the case, a more advanced type of dynamic treatment is most advantageous with varying transverse dose profile as a function of the angle of rotation. Such treatments are more difficult but can often be realized with treatment units using a multileaf collimator where each pair of opposed collimator leaves have to perform a complex motion [2] at every orientation of the gantry. Another possibility would be to use a set of fixed compensators

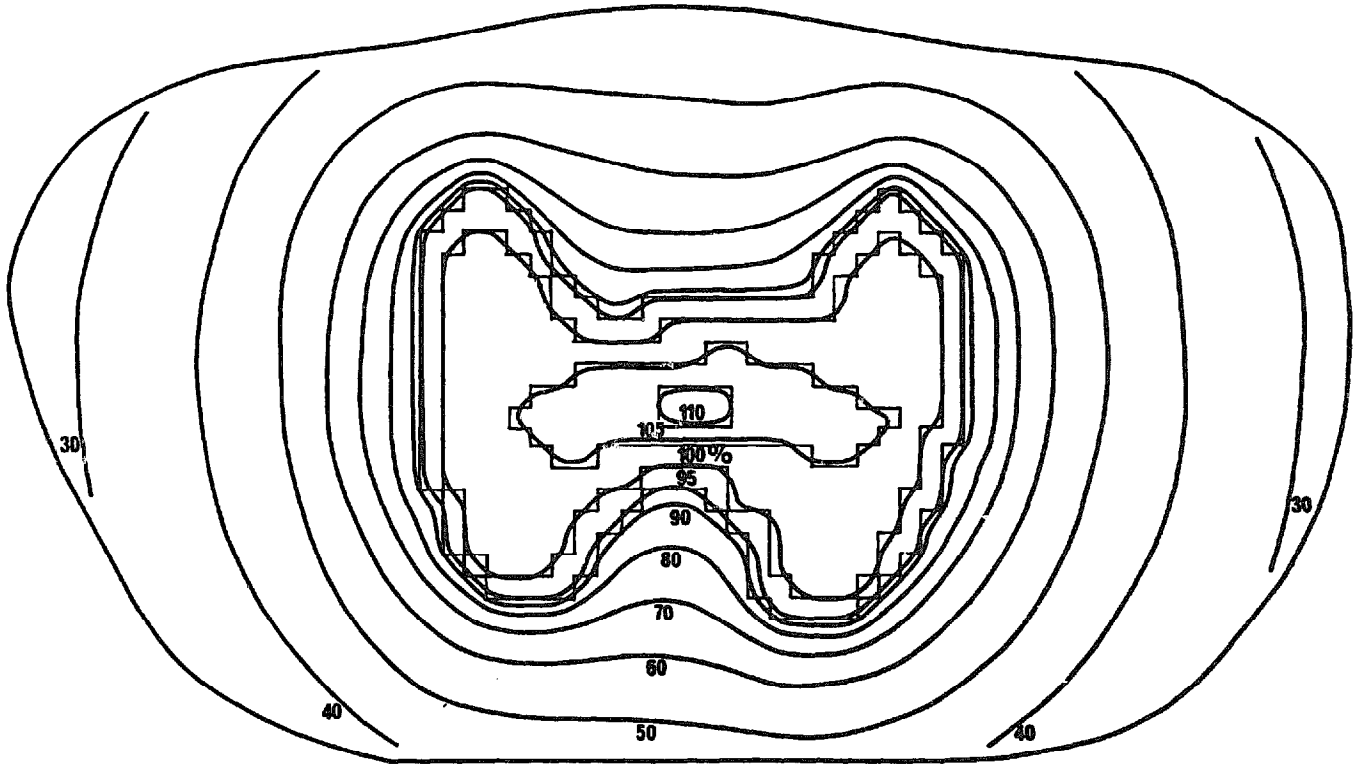

Fig. 5. The resultant dose distribution in the patient when using the target volume of Figs. 3 and 4 and the incident beams according to Fig. 4. It is seen that the isodoses very accurately follow the shape of the target volume which is defined by the 95% isodose.

and only irradiate from a small number of directions. A more general and flexible technique would be to use a beam flattening system based on scanned photon or electron beams [4,5,15,18] where the transversal dose distribution of the incident beam can be continuously varied during the rotation of the gantry as shown in Fig. 4.

Convex-concave target volumes with organs at risk

When the cross-section of the target volume in the plane of rotation deviates more and more from the simple convex shape [3], and in particular when there is an organ at risk in its vicinity (Fig. 6), the simple conformation type of treatment is no longer the best solution. This is because a conformation dose distribution will always be convex (see Fig. 7) and therefore the normal tissues outside the concave sections, where an organ at risk may be located, will receive unnecessarily high doses.

However, a generalization of the conformation technique may be possible. Instead of the traditional conformation approach, where each point in a convex target is irradiated from all directions, the angular interval under which each point is being irradiated is decreased by an angle* or, in the three dimensional case by, a double cone, δ (Fig. 6). This angle should preferably vary from point to point in the target volume but the average angular extention of the organ at risk as seen from all points in the target volume might be a sufficient compromise in many cases. This will reduce the dose at all points by the same amount and generate a depression in the azimutal distribution which could be oriented to minimize the dose to the organ at risk (shaded in Fig. 6). A more accurate and general approach which is applicable also with several organs at risk would be to reduce or switch off the irradiation of each point in the target volume over those angular intervals that may contain organs at risk. In both these cases, the value of the azimutally limited con-

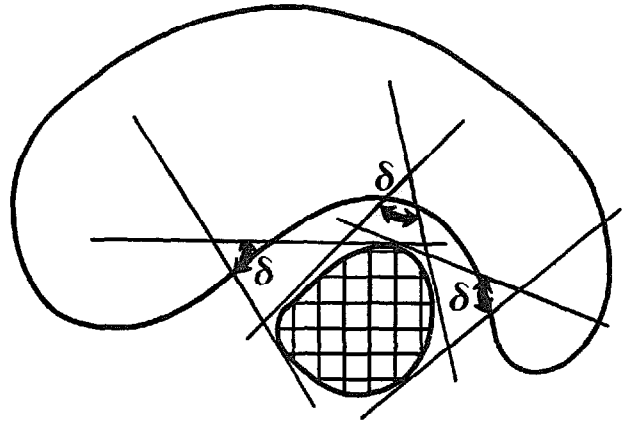

Fig. 6. When there is a very sensitive organ in the vicinity of the target volume, the best dose distribution is achieved by reducing the angle of irradiation at each point in the target by approximately an angle δ corresponding to the extension of the organ at risk (shaded).

vergent point irradiation distributions $d_a(\vec{r},\vec{r}_c)$ will depend both on the actual location of their center co-ordinates $\vec{r}_c$ and the location of the point of interest $\vec{r}$.

Quantitatively this type of irradiation could be formulated in analogy with Eqn. (9):

$$D(\vec{r}) = \int\int\int_{V_t} \varphi_a(\vec{r}_c)\, d_a(\vec{r},\vec{r}_c)\, d^3r_c \qquad (16)$$

where d_a now is the azimutally limited point irradiation distribution the value of which now will depend both on the location of its center point $\vec{r}_c$ and the field point of interest $\vec{r}$, not just their separation $(\vec{r} - \vec{r}_c)$. Unfortunately, this equation is therefore no longer a straight forward convolution but a more general so called Fredholm integral equation of the first kind. This equation is generally more difficult to solve even by numerically methods though a number of procedures are known [15,16,20]. Of special interest for computer applications are the iterative algorithms which avoid some of the problems with the Fourier transform technique discussed above, even though they may not be as fast as the latter. Among the special advantages of the iterative procedures are that they can be constrained, for example, in order to always

* A different but related investigation of the above problems with partly similar results has recently been made by Cormack [9].

generate non-negative dose distributions which is a trivial but necessary condition on the distribution. Practical applications of these equations will be presented in more details in proceeding publications.

Assuming now that an azimutally limited point irradiation density φ_a has been found which satisfies Eqn. (16). The optimal shape of the angular-dependent incident dose distribution that generates this density may again be determined by projection of $d_a \cdot \varphi_a$ on each position of the effective radiation source $\vec{r}_s$:

$$D(\xi,\eta,\theta) = \int_l d_a(\vec{r}_s,\vec{r}_c)\ \varphi_a(\vec{r}_c)\ e^{\mu_p z(\vec{r}_c)}\ dz \qquad (17)$$

where most of the notations are the same as in Eqn. (15). The main difference is that d_a will now switch the incident beam on or off depending on whether it will pass through an organ at risk.

The general technique described in the previous section for convex targets may in a modified form also be applicable to the present geometry provided the organ at risk is included in the target volume as a low or even a negative dose volume. It is important, however, that the negative dose specified in the risk organ is not too low such that the incident beam when determined from Eqn. (17) becomes negative. For the case of complete cylindrical symmetry, this problem has already been solved in a very general way [6,9].

A third alternative would be to analyze the desired dose distribution in terms of the even more elementary pencil beams [see Eqn. (6)]. However, this will increase the complexity of the equations due to the larger number of degrees of freedom. The advantage gained is that the most accurate optimization is obtained by this approach.

Discretization to a finite number of stationary beams

Today, when nearly all conventional radiation therapy treatment units are without scanning beam capabilities, it would be desirable to reduce the number of incident beams to a small number so ordinary beam compensators can be used.

A crude solution to this problem is to use just the inverse back-projections of $d \cdot \varphi$ on the desired directions. However, a more precise solution to this problem may be obtained by replacing the isotropic point irradiation density in Eqns. (9) and (16) with a point irradiation dose distribution d_n which only includes two, three or n pencil beams $p(\vec{r})$ which intercept at a common point. The directions and weights of the individual pencil beams can then be chosen to avoid irradiation of given organs at risk. By chosing this type of elementary point irradiation distribution the inverse back-projection will only require dose delivery from two, three or n different beam portals. This will greatly facilitate the use of ordinary beam compensators particularly when n is a small number as schematically illustrated in the lower line of Fig. 7.

In general, a larger number of incident beam directions are required when the desired dose distribution is more complicated for example as shown in Fig. 4. When the desired dose variations across the target volume are not too large, a rather small value for n should be acceptable. In general, it should be desirable to have the beams oriented such that a minimum of parallel opposed beams are obtained, for example, three beams at 120° intervals. The reason for this choice is that the resultant point irradiation distribution d_3 will be rather close to the optimal isotropic point irradiation distribution. In this way, the individual pencil beam exits partly fill the depressions between the opposed incident beams such that close to the convergence point the dose distribution is similar to that with six evenly spaced beams.

This result is quite interesting as it indicates that parallel opposed beam techniques should not be as advantageous as there frequent use may indicate. The principal reason for their popularity is of course that compensators are generally not required. In general, it should be more advantageous to use two oblique fields with wedge filters, for example, at 90° from each other or three fields as in Fig. 7 when more flexibility is required for shaping of the dose distribution inside the target volume.

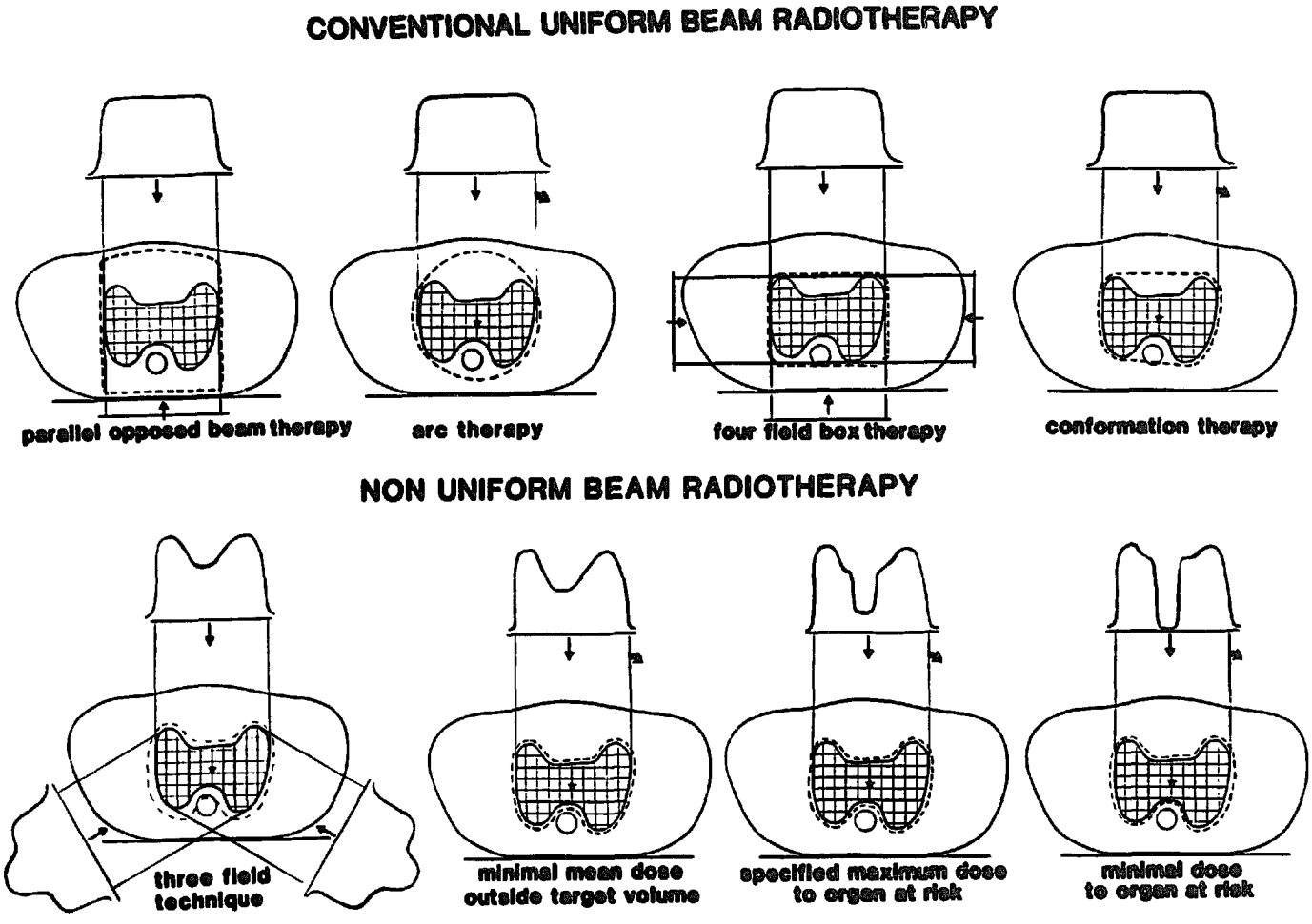

Fig. 7. Schematic comparison of different external beam irradiation techniques. It is seen that non-uniform dose delivery will in general allow a better matching of the treatment volume (-----) to the target volume (shaded).

Discussion

As seen from Fig. 4, the presently derived optimal irradiation techniques have many similarities with the back-projections used in computed tomography (CT). The main difference is that the negative valued filters used in CT reconstruction cannot be used in radiation therapy as the incident dose distributions by necessity are non-negative. The practical consequence of this fact is that arbitary dose distributions can not be delivered [6] whereas arbitary attenuation patterns can be determined using CT. For example, it is not possible to give a high dose to a volume in the patient and zero dose everywhere else.

In order to take this restriction into account, the desired dose distribution inside the target volume has here been analyzed in terms of the well known optimum dose distribution for the irradiation of a single point. The resultant point irradiation densities will therefore always be realizable and practicable and deliver minimum dose to surrounding normal tissues. The resulting irradiation technique generally will require a high dose to be delivered from directions where the incident beam passes a long distance through the target volume. In fact, with high energy beams or more specifically when the influence of beam attenuation and scatter is negligible, the optimal incident beam approaches a true geometric projection of the shape of the target volume. It is obvious that this will minimize the dose to surrounding normal tissues as the beams are used more effectively and there are generally less room for superficial normal tissues along the most heavily

weighted beam directions. When low megavoltage beams are used and the target volume has both narrow and broad sections, the point irradiation density will deviate substantially from the desired, often generally, uniform dose distribution as schematically illustrated in Fig. 4. The considerable influence of photon attenuation and scatter in this case will make the optimal incident beams deviate substantially from a pure geometrical projection of the target volume.

In order to illustrate the main properties of different external beam irradiation techniques with uniform and non-uniform incident beams, the target volumes (shaded areas) and treatment volumes (dashed lines) for a cervix tumor and associated lymph nodes are schematically illustrated in Fig. 7. It is clear from the figure that with strongly concave target volumes none of the uniform beam irradiation techniques can produce a concave treatment volume except to some extent for the fairly complex multicenter arc treatments. With non-uniform incident beams, the flexibility is much greater and even a two or three field technique will do the job as shown in the lower row.

Of special interest for the development of future dose planning techniques is that the best irradiation technique generally can be derived by deterministic methods using Fourier transform techniques or the solution of a Fredholm equation of the first kind. These methods may thus, in the near future, reduce the need for the time consuming trial and error approach often applied in dose planning of today. It will therefore be essential to develop computer algorithms for solving equations of the above type [e.g. Eqns. (9), (13), (16)] and develop suitable filter functions. Naturally the resultant dose profiles $D(\xi,\eta,\theta)$ will generally vary both laterally and with angle. Such developments will increase the need for computer controlled multileaf collimators preferably using scanned photon or electron beams to accomplish maximum flexibility in the shaping of the beam in each direction of the gantry [5,14,18].

Acknowledgements

Valuable help and suggestions by Dr. Bengt K. Lind are gratefully acknowledged. These investigations were in part supported by grants from the Swedish Medical Research Council.

References

1 Ahnesjö, A., Andreo, P. and Brahme, A. Calculation and application of point spread functions for treatment planning with high energy photon beams. Acta Radiol. Oncol. 26: 49–56, 1987.

2 Bjärngard, B.E. and Kijewski, P. The potential of computer control to improve dose distributions in radiation therapy. In: Computer Applications in Radiation Oncology, pp. 110–124. Editor: E.S. Sternick. University Press, New England, Hanover, NH, 1976.

3 Brahme, A. Optimal usage of multileaf collimators for stationary beam radiation therapy. Strahlenther. Oncol. in press, 1987.

4 Brahme, A. Design principles and clinical possibilities with a new generation of radiation therapy equipment. Acta Oncol., 26: 401–412, 1987.

5 Brahme, A., Kraepelin, T. and Svensson, H. Electron and photon beams from a 50 MeV Racetrack Microtron. Acta Radiol. Oncol. 19: 305–319, 1980.

6 Brahme, A., Roos, J.E. and Lax, I. Solution of an integral equation in rotation therapy. Phys. Med. Biol. 27: 1221–1229, 1982.

7 Brahme, A. and Svensson, H. Radiation beam characteristics of a 22 MeV microtron. Acta Radiol. Oncol. 18: 244–272, 1979.

8 Brahme, A. and Ågren, A.K. On the optimal dose distribution for eradication of heterogeneous tumours. Acta Oncol. 26: 377–385, 1987.

9 Cormack, A.M. A problem in rotation therapy with X-rays. Int. J. Radiat. Oncol. Biol. Phys. 13: 623–630, 1986.

10 Davies, A.R. On the maximum likelihood regularization of Fredholm convolusion equation of the first kind. In: Treatment of Integral Equations by Numerical Methods, pp. 95–105. Editors: C.T.H. Baker and G.S. Miller. Academic Press, New York, 1982.

11 Davison, B. Distributions in a non-absorbing body, of gamma-ray sources giving a uniform distribution of gamma-rays. Br. J. Radiol. (Suppl. 2) 197–198, 1950.

12 Du Sault, L.A. Simplified method of treatment planning. Radiology 77: 66–76, 1961.

13 Greeening, J.R. Fundamentals of Radiation Dosimetry. Hilger, Bristol, 1981.

14 Lind, B.K. and Brahme, A. Generation of desired dose distributions with scanned elementary beams by deconvolution methods. 7 ICMP Espoo, Finland, paper 4.10, p. 953, 1985.

15 Lind, B.K. and Brahme, A. Optimization of radiation therapy dose distributions using scanned electron and photon beams and multileaf collimators. In: Proc. 9th Int. Conf. on Computers in Radiation Therapy, pp. 235–239. Editors: I.A.D. Bruinvis, P.H. Van der Giessen and H.J. Van Kleffens, Elsevier, North-Holland, Amsterdam, 1987.

16 Miller, G.F. Fredholm equations of the first kind. In: Numerical Solutions of Integral Equations. Editors: L.M. Delves and J. Walsh. Claredon Press, TX, 1974.

17 Mohan, R., Chui, C.S. and Lidofsky, L. Differential pencil beam dose computation model for photons. Med. Phys. 13: 64, 1986.

18 Näfstadius, P., Brahme, A. and Nordell, B. Computer assisted dosimetry of scanned electron and photon beams for radiation therapy. Radiother. Oncol. 2: 261–269, 1984.

19 Roberts, J.E. Limiting factors of moving field dosimetry. In: Roentgens, Rads and Riddles, pp. 29–38. A.E.C., Washington DC, 1956.

20 Schafer, D.W., Mersereau, R.M. and Richards, M.A. Constrained iterative restoration algorithms. Proc. IEEE 69, 432–450, 1981.

21 Schoknecht, G. Die Beschreibung von Strahlenfeldern durch Separierung von Primär- und Streustrahlung. IV. Strahlentherapie 141: 326, 1971.

22 Tsien, K.C., Cunningham, J.R. and Wright, D.J. Effects of different parameters on dose distributions in Cobalt 60 planar rotation. Acta Radiol. Ther. Phys. Biol. 4: 129–154, 1966.